Nano-patterned glass superstrates with different aspect ratios for enhanced light harvesting in a-Si:H thin film solar cells

Ting-Gang Chen,[1] Peichen Yu,[1,*] Yu-Lin Tsai,[1] Chang-Hong Shen,[2] Jia-Min Shieh,[2] Min-An Tsai,[3] and Hao-Chung Kuo[1]

[1]*Department of Photonics and Institute of Electro-Optical Engineering, National Chiao Tung University, Hsinchu 30010, Taiwan*
[2]*National Nano Device Laboratories, Hsinchu 30078, Taiwan*
[3]*Industrial Technology Research Institute, Hsinchu 31040, Taiwan*
[*] *yup@faculty.nctu.edu.tw*

Abstract: Nano-patterned glass superstrates obtained via a large-area production approach are desirable for antireflection and light trapping in thin-film solar cells. The tapered nanostructures allow a graded refractive index profile between the glass and material interfaces, leading to suppressed surface reflection and increased forward diffraction of light. In this work, we investigate nanostructured glass patterns with different aspect ratios using scalable nanosphere lithography for hydrogenated amorphous silicon (a-Si:H) thin film solar cells. Compared to flat glass cell and Asahi U-type glass cell, enhancements in short-circuit current density (J_{sc}) of 51.6% and 8%, respectively, were achieved for a moderate aspect ratio of 0.16. The measured external quantum efficiencies (EQE) spectra confirmed a broadband enhancement due to antireflection and light trapping properties.

OCIS codes: (310.6628) Subwavelength structures, nanostructures; (040.5350) Photovoltaic.

References and links

1. R. F. Service, "Solar energy. Can the upstarts top silicon?" Science **319**(5864), 718–720 (2008).
2. A. V. Shah, H. Schade, M. Vanecek, J. Meier, E. V. Sauvain, N. Wyrsch, U. Kroll, C. Droz, and J. Bailat, "Thin-film silicon solar cell technology," Prog. Photovolt. Res. Appl. **12**, 113–142 (2004).
3. C. Haase and H. Stiebig, "Optical properties of thin-film silicon solar cells with grating couplers," Prog. Photovolt. Res. Appl. **14**, 629–641 (2006).
4. C. Eisele, C. E. Nebel, and M. Stutzmann, "Periodic light coupler gratings in amorphous thin film solar cells," J. Appl. Phys. **89**, 7722–7726 (2001).
5. C. Ulbrich, M. Peters, B. Bläsi, T. Kirchartz, A. Gerber, and U. Rau, "Enhanced light trapping in thin-film solar cells by a directionally selective filter," Opt. Express **18**(Suppl 2), A133–A138 (2010).
6. T. Tiedje, B. Abeles, J. M. Cebulka, and J. Pelz, "Photoconductivity enhancement by light trapping in rough amorphous silicon," Appl. Phys. Lett. **42**, 712–714 (1983).
7. J. C. Lee, V. Dutta, J. S. Yoo, J. S. Yi, J. S. Song, and K. H. Yoon, "Superstrate p-i-n a-Si:H solar cells on textured ZnO: Al front transparent conduction oxide," Superlattices Microstruct. **42**, 369–374 (2007).
8. H. Sai, H. Jia, and M. Kondo, "Impact of front and rear texture of thin-film microcrystalline silicon solar cells on their light trapping properties," J. Appl. Phys. **108**, 044505 (2010).
9. J. Krc, B. Lipovsek, M. Bokalic, A. Campa, T. Oyama, M. Kambe, T. Matsui, H. Sai, M. Kondo, and M. Topic, "Potential of thin-film silicon solar cells by using high haze TCO superstrates," Thin Solid Films **518**, 3054–3058 (2010).
10. Y. Li, J. Zhang, S. Zhu, H. Dong, F. Jia, Z. Wang, Z. Sun, L. Zhang, Y. Li, H. Li, W. Xu, and B. Yang, "Biomimetic surfaces for high-performance optics," Adv. Mater. (Deerfield Beach Fla.) **21**, 4731–4734 (2009).
11. J. Zhu, C. M. Hsu, Z. Yu, S. Fan, and Y. Cui, "Nanodome solar cells with efficient light management and self-cleaning," Nano Lett. **10**(6), 1979–1984 (2010).
12. C. Battaglia, C. M. Hsu, K. Söderström, J. Escarré, F. J. Haug, M. Charrière, M. Boccard, M. Despeisse, D. T. L. Alexander, M. Cantoni, Y. Cui, and C. Ballif, "Light trapping in solar cells: can periodic beat random?" ACS Nano **6**(3), 2790–2797 (2012).
13. C. H. Chiu, P. Yu, H. C. Kuo, C. C. Chen, T. C. Lu, S. C. Wang, S. H. Hsu, Y. J. Cheng, and Y. C. Chang, "Broadband and omnidirectional antireflection employing disordered GaN nanopillars," Opt. Express **16**(12), 8748–8754 (2008).

#164585 - $15.00 USD Received 13 Mar 2012; revised 5 Apr 2012; accepted 8 Apr 2012; published 12 Apr 2012

14. Y. H. Pai, Y. C. Lin, J. L. Tsai, and G. R. Lin, "Nonlinear dependence between the surface reflectance and the duty-cycle of semiconductor nanorod array," Opt. Express **19**(3), 1680–1690 (2011).
15. H. Li, R. H. Franken, R. L. Stolk, J. A. Schuttauf, C. H. M. van der Werf, J. K. Rath, and R. E. I. Schropp, "On the development of single and multijunction solar cells with hot-wire CVD eposited active layers," J. Non-Cryst. Solids **354**, 2445–2450 (2008).
16. P. Doshi, G. E. Jellison, and A. Rohatgi, "Characterization and optimization of absorbing plasma-enhanced chemical vapor deposited antireflection coatings for silicon photovoltaics," Appl. Opt. **36**(30), 7826–7837 (1997).

1. Introduction

Silicon-based photovoltaics are promising due to their long-term stability and the availability of non-toxic, abundant material resources [1]. Although silicon is an indirect bandgap material, hydrogenated amorphous silicon (a-Si:H) has disordered atomic structures with an absorption coefficient that is two orders larger than that of crystalline silicon in the visible spectrum. Such a typical a-Si:H cell exhibits potential for light-weight, flexible, and cost-effective production. In general, the thickness of the a-Si:H cells presents a tradeoff between sufficient light absorption and minority carrier collection. Therefore, light trapping schemes which increase the optical path length and the possibility of total internal reflection are imperative to a-Si:H solar cells [2–4].

In general, there exist two device configurations of a-Si:H thin film solar cells. For the substrate (n-i-p) type, first the n-type active material is grown from a textured back reflector, followed by the growth of an intrinsic and p-type a-Si:H layer, a transparent-conductive-oxide (TCO) layer, and a frontal metal grid [5, 6]. In the superstrate (p-i-n) type, the growth order of active materials is reversed and the p-type material is first deposited on a textured TCO coated glass where light enters [7]. For both types, surface texturing is employed to scatter the incident light, particularly for weakly absorbed photons with a wavelength near the optical bandgap. By virtue of a conforming growth mechanism, the front or rear textures are carried to the opposite surface. However, front and rear surface textures may benefit the device characteristics in very different ways. The light trapping introduced by the rear textures only improves the optical absorption in the long-wavelength spectral range and is unlikely to avoid the parasitic loss due to metal absorption and back surface recombination [8, 9]. In contrast, the frontal textures have the same ability to scatter incident light at the entrance, with an additional benefit whereby the rough surface could reduce the surface reflection, leading to broadband enhancements of light absorption.

In this work, a front side surface texture configuration is adopted by directly patterning the glass superstrates using polystyrene nanosphere lithography and reactive-ion etching techniques for large-area production [10]. Nanoscale patterned glass is desirable due to a graded refractive index profile between the glass and a-Si:H interfaces, leading to a suppressed surface reflection. Moreover, the nanostructures also enhance the diffraction of light, further increasing the equivalent optical absorption path of a-Si thin film solar cells [11, 12]. Since it has been reported that the surface reflection properties of the nano-scale patterns are highly correlated with the aspect ratios with a periodicity near the wavelength of interest [13, 14], herein we investigate the optical and electrical properties of a-Si:H thin film solar cells fabricated on nano-patterned glass with various aspect ratios. The results indicate that the optical absorption of the a-Si:H layer increases with increasing aspect ratios due to their broadband absorption. Nevertheless, the electrical properties are restricted by steep surface roughness [15]. Enhanced photovoltaic characteristics are demonstrated for the nanostructured glass superstrate with a moderate aspect ratio of 0.16. Compared to flat and Asahi U-type glass cells, respectively, the short-circuit current density (J_{sc}) achieved 51.6% and 8% enhancement and the power conversion efficiency (PCE) achieved 48.4% and 3.1% enhancement. The external quantum efficiency spectra confirmed a broadband enhancement due to antireflection and light trapping properties. The present concept of patterned glass with only 80 nm of TCO is a potential cost reduction strategy for various types of thin film solar cells, such as CdTe thin film cells, organic solar cells, and so on.

#164585 - $15.00 USD Received 13 Mar 2012; revised 5 Apr 2012; accepted 8 Apr 2012; published 12 Apr 2012

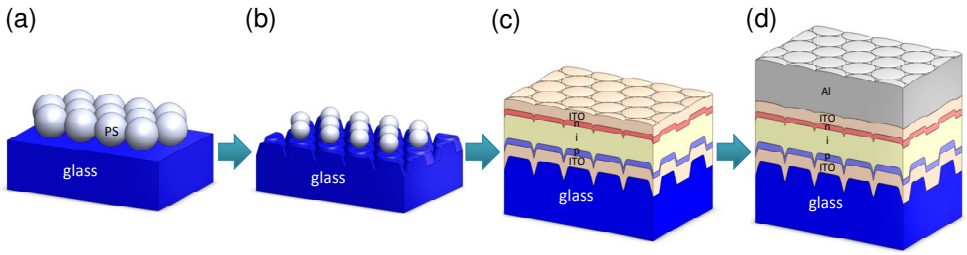

Fig. 1. The schematic fabrication process for patterned glass a-Si:H thin film solar cells. (a) The hexagonal array of closely packed polystyrene nanospheres was first formed on glass. (b) RIE was involved for etching the glass superstrate. (c) The front ITO and p-i-n a-Si:H stacks were subsequently deposited on glass superstrate. An 80 nm ITO served as a back contact to reduce series resistance. (d) A 1000 nm Al was evaporated as a back reflector.

2. Fabrication

The patterned glass superstrate was fabricated using polystyrene nanosphere lithography followed by reactive-ion etching (RIE) techniques as illustrated in Fig. 1. First, polystyrene nanospheres were self-assembled in an alcohol and water mixture, forming close-packed hexagonal arrays. The glass superstrate was first dip-coated with nanospheres as the sacrificial mask and subsequently dry-etched under CF_4:Ar gas flow rates of 30:20 sccm with an RF power of 250 W and a chamber pressure of 40 mTorr. The etching rate was about 0.45 nm per second. The remaining polystyrene nanospheres were then removed in a boiling H_2O_2/H_2SO_4 solution. Afterwards, an 80 nm thick indium-tin-oxide (ITO) frontal electrode was sputtered on the glass superstrate. We employed a very high frequency chemical vapor deposition (VHF-CVD) system operating at a frequency of 40 MHz to deposit the a-Si:H layer. The thicknesses of the doped and intrinsic a-Si:H p-i-n stacks were 15, 400, and 20 nm, respectively. Afterward, a reflective back contact of ITO/Al was sputtered and electron-beam evaporated with thicknesses of 80 nm and 1000 nm respectively with a shadow mask. Isolation was performed by etching away the unprotected area defined by Al, resulting in a cell area of 5 mm × 5 mm. Meanwhile, a flat glass with an 80 nm thick ITO layer and a commercially available Asahi U-type glass consisting of an 800 nm thick SnO_2:F electrode with surface textures of ~200 nm random pyramids were also fabricated as references for comparison.

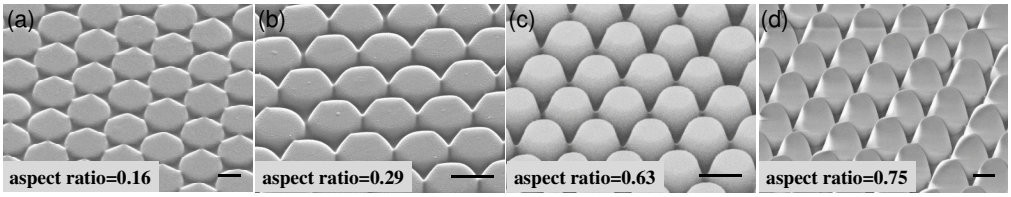

Fig. 2. (a)–(d) Tilted 45 degree SEM images of patterned glass superstrates with aspect ratios of 0.16, 0.29, 0.63, and 0.75, respectively. The scale bar represents 1 μm in length.

To realize the dimensional limits of nano-patterned glass for an a-Si:H cell, the dependence of cell performances on the surface morphology was investigated by fabricating nanostructures with various dimensions. We employed polystyrene nanospheres with two different diameters and etched the samples with two different RIE times to generate samples with four different aspect ratios. The bottom diameters of patterns for four individual samples are 960, 590, 590, and 960 nm with corresponding heights of 160, 170, 370, and 720 nm, respectively. The structures are described by aspect ratios, defined as the height divided by the diameter with calculated standard deviations as error ranges: 0.16 ± 0.01, 0.29 ± 0.02, 0.63 ± 0.04, and 0.75 ± 0.04, respectively. The morphology of the nano-patterned glass was examined using a scanning electron microscope (SEM). Figures 2(a)–2(d) show the tilted 45

#164585 - $15.00 USD Received 13 Mar 2012; revised 5 Apr 2012; accepted 8 Apr 2012; published 12 Apr 2012

degrees views of the nano-patterned glass with aspect ratios of 0.16, 0.29, 0.63, and 0.75, respectively. The nano-discs are arranged in a close-packed hexagonal array.

Figure 3(a) shows the rear side morphology of a complete a-Si:H cell after the final Al evaporation. The image indicates that frontal glass patterns were successfully transferred to the back surface. Figure 3(b) shows the cross-sectional SEM image of a fabricated a-Si:H solar cell on the patterned glass superstrate with an aspect ratio of 0.75. It is observed that large air gaps appear at a-Si:H layer and the Al are blocked on top. Figure 3(c) shows the cross-sectional transmission electron microscopic (TEM) image of an a-Si:H cell fabricated on a Asahi-U type glass superstrate with a frontal textured electrode.

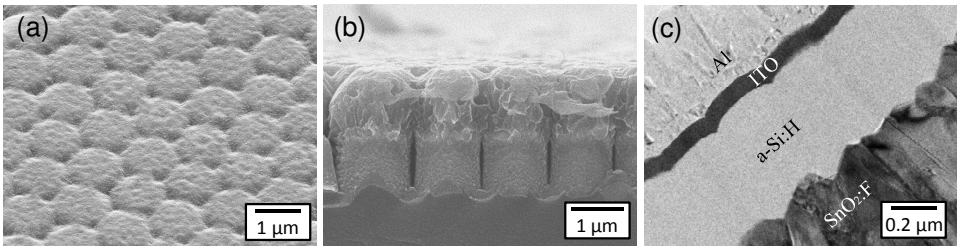

Fig. 3. (a) The SEM image of the rear surface morphology of a complete a-Si:H cell with a patterned glass with an aspect ratio of 0.16 after Al covering. (b) Cross-sectional SEM image of a patterned glass with an aspect ratio of 0.75 showing air gaps between patterns. (c) The TEM image of an Asahi-U type a-Si:H cell with a textured SnO_2:F electrode.

To better understand the morphologies of material deposition on differently textured substrates, the TEM samples were prepared for aspect ratios of 0.16 and 0.75. As shown in Fig. 4(a) and an enlarged view in 4(b), a conformal growth of ITO, active layers, and Al is observed on the glass pattern with aspect ratio of 0.16. The first 15 nm p-layer can be smoothly deposited down to the valleys. However, some striped voids appear from the valleys during the deposition of the a-Si:H i-layer. On the other hand, as shown in Fig. 4(c) and 4(d), the ITO and a-Si:H layers cannot be conformably grown on the glass pattern with an aspect ratio of 0.75, adding difficulties to control the layer thickness. Moreover, the large striped voids between patterns may introduce a shunting path and worsen the device performance.

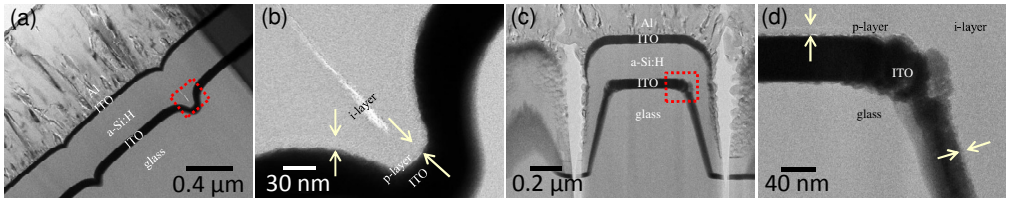

Fig. 4. (a) Cross-sectional TEM image of a cell deposited on the patterned glass with an aspect ratio of 0.16, and (b) an enlarged image of the red frame indicated in (a). Yellow arrows mark the 15 nm thick p-layer. (c) A cell deposited on a patterned glass with an aspect ratio of 0.75, showing non-conformal growth of ITO and the a-Si:H layers and (d) an enlarged image of the red frame in (c), indicating a flimsy p-layer on the sidewall.

3. Measurement and analysis

To characterize the optical properties of a-Si:H solar cells on flat and patterned glass superstrates, the reflectance spectra were measured using an integrating sphere at normal illumination incidence. Figure 5(a) shows the reflectance spectra for samples with various aspect ratios. Compared to a flat glass cell, the patterned glass cell shows broadband antireflection and absorption which is positively correlated with the aspect ratio for wavelengths above 550 nm. For wavelengths below 550 nm, light could be completely absorbed by a-Si:H within a round trip in the presence of the back reflector. Therefore, the low reflectance below 550 nm reveals a prominent antireflective property that surpasses the Asahi U-type glass counterpart. For wavelengths above 550 nm, the optical path length

#164585 - $15.00 USD Received 13 Mar 2012; revised 5 Apr 2012; accepted 8 Apr 2012; published 12 Apr 2012

depicted by the thickness of active layers is shorter than the required absorption length. Therefore, the frontal nano-patterned glass shows significantly suppressed reflectance due to both antireflection and light trapping, which increase the optical absorption.

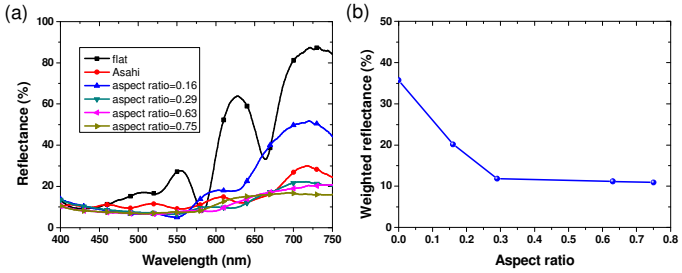

Fig. 5. (a) The reflectance spectra for the flat reference, Asahi U-type glass, and patterned glass a-Si:H cells with various aspect ratios. (b) The AM1.5G solar spectrum weighted reflectance as a function of aspect ratios.

To further evaluate the light harvesting capability of the a-Si:H solar cell with respect to the aspect ratio, the AM1.5G-solar-spectrum-weighted reflectance was calculated using the equation from Ref [16]. with the measured reflectance spectra. Figure 5(b) shows the weighted reflectance as a function of pattern aspect ratios. The results indicate that the weighted reflectance is significantly reduced from 36% with the flat glass reference to 20% with the patterned glass that has an aspect ratio of 0.16 and saturated at 11% for nano-patterns with aspect ratios larger than 0.29.

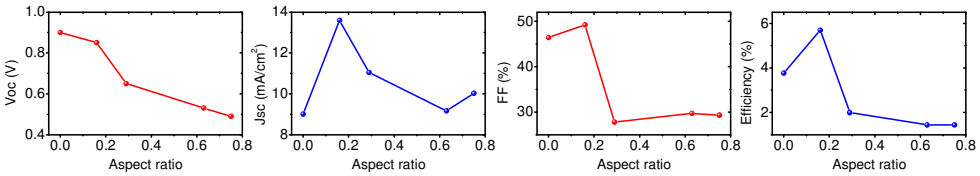

Fig. 6. The solar cell characteristics of patterned glass superstrates as a function of aspect ratios.

The current density–voltage (J-V) characterizations were performed using a standard solar simulator with an illumination condition of 1000 W/m^2 for the AM1.5G solar spectrum. As shown in Fig. 6, the short-circuit current density (J_{sc}) is higher than its flat glass counterpart with an aspect ratio equal to zero for all samples. However, clear decreasing trends of the open-circuit voltage (V_{oc}), fill factor (FF), and efficiencies with increasing aspect ratios larger than 0.16 are also observed. Moreover, the J_{sc} values also counteract the trend of the weighted reflectance in which the sample with a higher aspect ratio achieves more absorption of light. Since the first p-type a-Si:H layer is only 15 nm thick, abrupt textures with an extensive surface area encounter issues such as film uniformity, coverage, and defects as leakage paths for photogenerated carriers as shown in Fig. 4(c) and 4(d). Moreover, due to the anisotropic deposition of a-Si:H, the rough textures with sharp angles result in the appearance of voids during deposition. As a result, these properties aggravate the recombination and degrade the cell performance even though the optical absorption is improved. The experimental results suggest nano-glass patterns with a moderate aspect ratio of 0.16 could extract the maximum photocurrent without significantly degrading the carrier collection.

The best performing patterned glass a-Si:H cell with an aspect ratio of 0.16 was compared with the flat and Asahi U-type superstrate cells. The cell characteristics were measured and are summarized in Table 1. As shown in Fig. 7(a), the V_{oc} is slightly lower for the patterned glass cell than for the flat glass counterpart due to higher recombination, but it is still comparable to Asahi U-type glass with different TCO materials. The fill factors show no significant differences between these three superstrates. It is worth mentioning that the patterned glass cell with an 80 nm thick frontal ITO contact is only a tenth of the thickness of

#164585 - $15.00 USD Received 13 Mar 2012; revised 5 Apr 2012; accepted 8 Apr 2012; published 12 Apr 2012

an Asahi U-type glass using 800 nm SnO_2:F TCO. The data on short-circuit current density, the patterned glass exhibits enhancements of 51.6% and 8% compared to the flat and Asahi U-type glasses, respectively, with overall enhancements in power conversion efficiency of 48.4% and 3.1%, respectively. All cells of the three different superstrates were fabricated side-by-side at the same time to ensure the same deposition conditions for comparison.

Table 1. Current Density–Voltage Characteristics of a-Si:H Solar Cells with Different Superstrates

Type	V_{oc} (V)	J_{sc} (mA/cm^2)	FF (%)	η (%)
Flat glass	0.90	9.01	46.40	3.76
Asahi U-type	0.87	12.62	50.03	5.49
Patterned glass	0.85	13.62	49.19	5.69

To better analyze the nature of the J_{sc} increment, the spectral responses were obtained by scanning a monochromatic beam from a Xenon lamp and are shown in Fig. 7(b). The IQE spectra can be calculated using the expression: IQE = EQE/(1-R) as shown in Fig. 7(c). The trend of the measured EQE spectra of the patterned glass cell and the Asahi U-type glass cell agree with the reflectance spectra shown in Fig. 5(a). Moreover, it can also be seen in Fig. 7(c) that the patterned glass cell shows a clear IQE improvement over the Asahi-U type cell for wavelengths between 400nm and 640nm due to variations of the p-layer thickness on different surface textures and a reduced usage of the frontal transparent conductive oxide material, which accounts for approximately 2-3% parasitic absorption loss in the visible and near infrared wavelength regimes [9]. Therefore, we think that the IQE improvement of the patterned glass cell is partially attributed to the reduced absorption loss of the frontal electrode, as well as a consequence of the p-layer thickness variation by growing the cells on substrates with different textures.

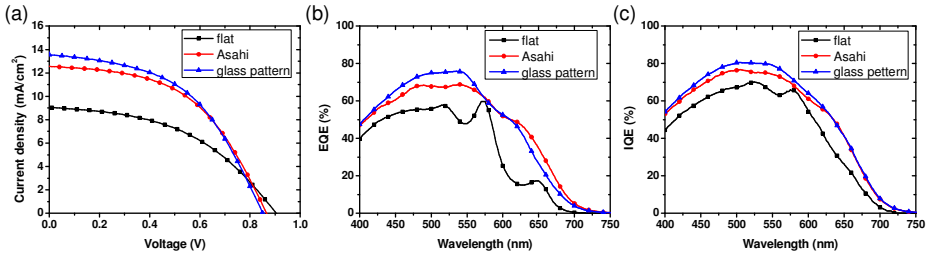

Fig. 7. (a) The current density–voltage characteristics under one sun AM1.5G illumination, (b) the corresponding EQE spectra, and (c) calculated IQE spectra.

4. Conclusion

In conclusion, nano-patterned glass a-Si:H solar cells have been demonstrated by employing polystyrene nanosphere lithography and reactive-ion etching techniques. The patterned glass cell with an aspect ratio of 0.16 shows short-circuit current density enhancements of 51.6% and 8% and power conversion efficiency enhancements of 48.4% and 3.1%, respectively, compared to flat glass and Asahi U-type glass superstrate cells. The measured EQE spectra reveal a broadband antireflection property and combined light trapping for wavelengths above 550 nm. To obtain overall enhancements of power conversion efficiency, the patterned glass with a high aspect ratio should be avoided due to its degraded electrical properties. The patterned glass superstrate with an 80 nm ITO electrode shows great potential for low-cost and high efficiency a-Si:H solar cells and can also be adopted for other thin film techniques.

#164585 - $15.00 USD Received 13 Mar 2012; revised 5 Apr 2012; accepted 8 Apr 2012; published 12 Apr 2012